

pubs.acs.org/Macromolecules Article

Mechanism of Initiation Stereocontrol in Polymerization of *rac*-Lactide by Aluminum Complexes Supported by Indolide—Imine Ligands

Anna M. Luke, Appie Peterson, Sina Chiniforoush, Mukunda Mandal, Yanay Popowski, Hussnain Sajjad, Caitlin J. Bouchey, Dimitar Y. Shopov, Brendan J. Graziano, Letitia J. Yao, Christopher J. Cramer, Theresa M. Reineke, and William B. Tolman*



Cite This: https://dx.doi.org/10.1021/acs.macromol.0c00092



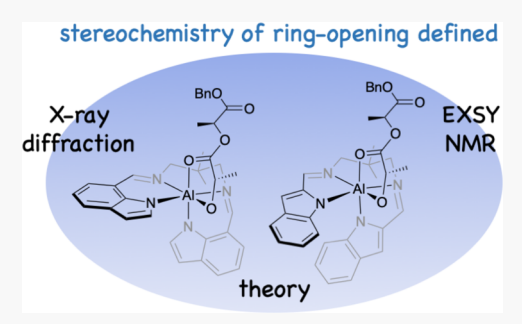
ACCESS

Metrics & More

Article Recommendations

s Supporting Information

ABSTRACT: The solid state and fluxional behaviors in solution of complexes L²AlOBn and L⁷AlOBn (Bn = benzyl) supported by an analog of salen incorporating indolide arms connected via their 2- and 7-positions were defined by experiment and theory. The complexes catalyze the stereoselective conversion of *rac*-lactide (*rac*-LA) to isotactically enriched polylactide. A key aspect of the stereocontrol was examined through study of the initiation reactions via NMR spectroscopy, X-ray crystal structures of the ring-opened products, and theory. The results include the first unambiguous structural definition of stereocontrol in ring-opening of LA by a metal—alkoxide complex and the finding that definition of the stereochemistry of initiation by the studied system is governed thermodynamically rather than kinetically.



INTRODUCTION

An important goal of contemporary research is to develop catalysts capable of polymerizing bioderived monomers with high selectivity, good molecular weight (MW) control, fast and/or convenient rates, and sufficient robustness to operate under potentially useful and/or industrially relevant conditions. The stereoselective ring-opening transesterification polymerization (ROTEP) of racemic lactide (rac-LA) to yield polylactide (PLA) has been particularly well-studied² because of the utility of PLA in a wide range of applications and the importance of PLA tacticity in determining its properties.³ Among the plethora of catalysts examined for this purpose, (salen)AlOR complexes (Figure 1) have garnered considerable attention due to their high MW control, rates convenient for NMR spectroscopic monitoring, and ease of synthesis of ligand derivatives, with several having engendered high stereoselectivity in polymerizations of rac-LA.⁴ While this previous work has provided considerable insight, detailed molecularlevel mechanistic understanding is limited, and further work is needed to address such issues as the impact of supporting ligand structural features on polymerization behavior, the specific molecular basis for observed stereocontrol using both chiral and achiral supporting ligands, and the precise structures of key intermediates. Such understanding is of potential utility for future catalyst design.

Recently, we reported predictions by theory of cyclic ester polymerization efficiency for a series of aluminum catalysts, including the complex L⁷AlOBn supported by a novel analog

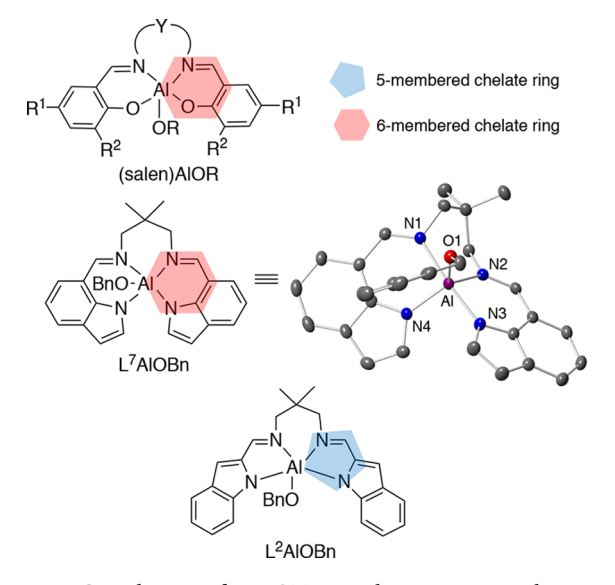


Figure 1. Complexes used as ROTEP catalysts. X-ray crystal structure reported in ref 5 (Λ isomer shown).

Received: January 14, 2020

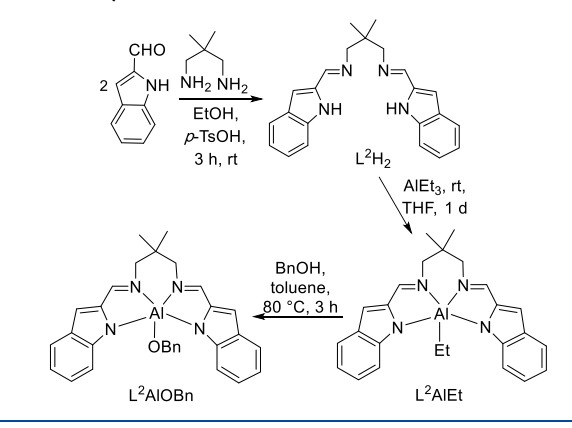
of salen incorporating indolide arms connected at their 7-position (Figure 1). Subsequent synthesis of L⁷AlOBn and studies of the kinetics of ROTEP of ε -caprolactone by the complex confirmed the prediction, validating the theoretical approach toward catalyst design. In that work, the X-ray crystal structure of the complex revealed a chiral structure with the ligand twisted such that the indolide rings are inequivalent. NMR spectroscopy showed the rings to be equivalent, however, suggesting operation of a fluxional process in solution. In view of these structural attributes and analogies to efficacious (salen)AlOR systems (for example, (TBSsalen)-AlOR, with Y = CH₂CMe₂CH₂, R¹ = H, R² = tBuMe₂Si), And we hypothesized that L⁷AlOBn might exert stereocontrol in ROTEP of rac-LA.

Herein, we describe evaluation of the fluxionality of L⁷AlOBn in solution by variable temperature (VT) NMR spectroscopy, theory, and studies of the ROTEP of rac-LA by the complex. Also, we compare its structural features and reactivity to an analogous complex L²AlOBn in which the indolide rings are connected at the 2- rather than the 7position to yield 5- instead of 6-membered chelate rings (Figure 1).6 As this work was being completed, the synthesis and use of L²AlOiPr in stereoselective polymerizations of LA, as well as the identification of a ring-opened LA complex, were reported, but the rationale for selectivity in ROTEP was not studied.7 In our work, through synergistic theoretical and experimental approaches, the effects of the supporting ligand differences on the ROTEP behavior of L²AlOBn and L⁷AlOBn were evaluated, with a specific emphasis on understanding the basis of the observed stereocontrol in the first ring-opening step (initiation) of rac-LA. Among our findings are precise structural determinations by X-ray crystallography of the initial products of ring-opening of rac-LA by metal-alkoxide complexes, revealing the stereochemistry of initiation. In addition, we evaluated said initiation by two-dimensional NMR spectroscopy and theory, leading to new insights into the basis for stereoselectivity and a key finding of thermodynamic rather than kinetic governance of stereocontrol. These studies, placed in perspective through comparisons to (salen)AlOR systems and, more broadly, to many other catalysts, ^{2,4} provide deep mechanistic understanding of ROTEP reactions of importance for sustainable polymer synthesis.

■ RESULTS AND DISCUSSION

Synthesis and Characterization of Complexes. The complex L7AlOBn was prepared as described previously5 and the synthesis of L²AlOBn was performed similarly (Scheme 1).7 Thus, condensation of indole-2-carboxaldehyde and 2,2dimethyl-1,3-propanediamine yielded L²H₂ (56%, Figure S1), which upon metalation with AlEt₃ afforded L²AlEt (98%); the characterization data for this complex matched that reported elsewhere.⁷ Subsequent reaction with BnOH yielded L²AlOBn (80%). Both L²AlOBn and L⁷AlOBn were characterized by CHN analysis and NMR spectroscopy, as well as X-ray crystallography, here for the former (Figures 2, S2, and S3). The structure features distorted trigonal bipyramidal geometry, with a τ_5 value⁸ of 0.62 (theory: 0.68) similar to that reported for L²AlOiPr (0.65). By comparison, the values for L⁷AlOBn⁵ and (TBSsalen)AlOBn4n are 0.87 and 0.83, respectively, indicating geometries closer to ideal trigonal bipyramidal for these complexes. Each of the complexes crystallizes as a mixture of enantiomers; for the complexes of (L2)2- and (L⁷)²⁻, the ligand in each stereoisomer is twisted so that the

Scheme 1. Syntheses of L²AlEt and L²AlOBn



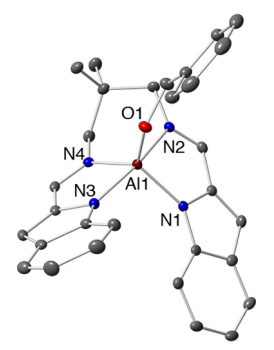


Figure 2. Representation of the X-ray crystal structure of L^2AlOBn , showing one enantiomer (Δ) of the two present in the unit cell as 50% ellipsoids with H atoms omitted for clarity. Selected bond distances (Å) and angles (degrees): Al1–O1, 1.722(3); Al1–N1, 1.939(0); Al1–N2, 2.003(9); Al1–N3, 2.069(8); Al1–N4, 1.918(5); N2–Al1–N3, 81.915(0); N2–Al1–N4, 113.075(1); N2–Al–O1, 126.132(1); N4–Al1–O1, 110.979(8); N4–Al1–N3, 81.751(9); N1–Al1–O1, 96.337(2); N3–Al1–O1, 96.506(9); N4–Al1–N1, 101.061(2); N2–Al1–N1, 81.750(5); N3–Al1–N1, 163.179(9).

indolide rings are inequivalent, with the enantiomers differentiated by the indolide ring orientation (labeled as Δ or Λ as indicated in Chart 1).

The inequivalence of the indolide rings in the X-ray structures of L²AlOBn and L⁷AlOBn is not reflected in their ¹H NMR spectra at 300 K, as only one set of peaks for the indolide and imine hydrogen atoms is observed (Figure 3 and

Chart 1. Enantiomers of Complexes L⁷AlOR and L²AlOR (R = Bn), with Labeling of Chirality Indicated

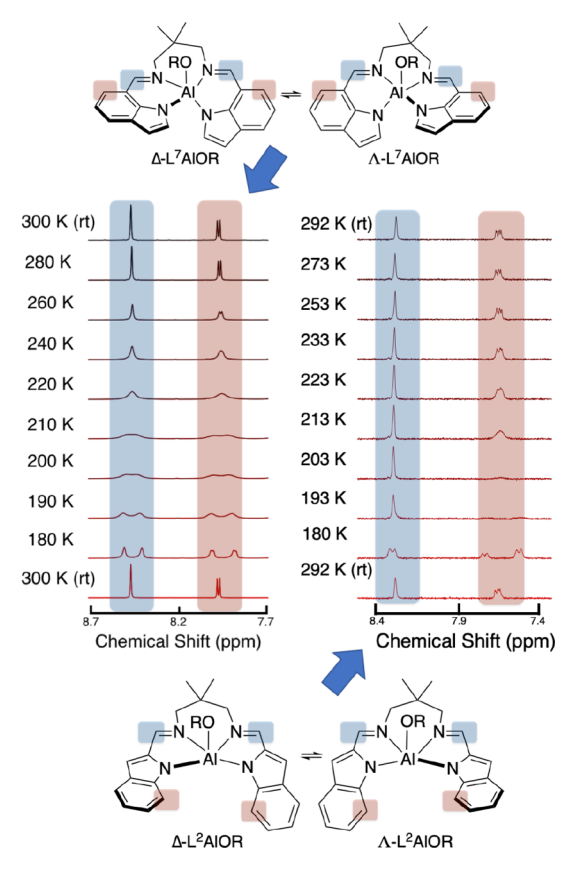


Figure 3. Selected VT-NMR (1 H) data for L 7 AlOBn (left) and L 2 AlOBn (right) with proposed assignments. The bottom spectra were collected after returning to rt to show reversibility. Full spectra are shown in Figures S11 and S13.

S3). This observation suggests a fluxional process that interconverts the indolide ring environments and is sufficiently rapid on the NMR time scale to result in averaging of the associated peaks. This hypothesis was confirmed through VT-NMR experiments for both complexes (Figures 3, S11 and S13). Illustrative peaks for the hydrogen atoms on the imine and the 6-position of the indolide rings for L⁷ and 7-position for L² undergo reversible decoalescence to yield a peak pattern indicative of inequivalent indolide rings upon lowering the temperature. Spectral fitting and Eyring analyses (Figures S15 and S16 and Table S1) yielded $\Delta G^{\ddagger}_{298 \text{ K}} = 10.2 \text{ kcal mol}^{-1}$ and 10.7 kcal mol⁻¹ for the processes for L⁷AlOBn and L²AlOBn, respectively. As similar fluxionality had been proposed for (salen)AlOR complexes (Figure 1),4n we prepared (TBSsalen)AlOBn according to the literature procedure⁴ⁿ and through VT-NMR studies determined $\Delta G^{\ddagger}_{298 \text{ K}}$, which was similar (9.0 kcal mol⁻¹).

Hypothesizing that the fluxionality observed in solution derived from interconversion of the Δ and Λ enantiomers of the complexes (Figure 3), we performed DFT calculations to interrogate the process. After a thorough conformational search to find all the low-lying conformers of L²AlOBn and L7AlOBn, the barrier for chirality inversion for the complexes was then found through optimizing the transition state structures. The barriers found for the complexes were similar (L7AlOBn = 9.9 kcal mol⁻¹; L²AlOBn = 11.6 kcal mol⁻¹) and agreed closely with those found experimentally (10.2 and 10.7 kcal mol⁻¹, respectively). For L7AlOBn, the lowest energy conformer has a twist-boat-like conformation in the six-

membered metallacycle formed by the Al atom and the ligand backbone, whereas in the transition state, the metallacycle has a more symmetric chair-like conformation. As a result, the fluxional process happens in two steps, involving conformational change of the metallacycle followed by movement of the rings into the more symmetric transition state (Figure 4). For

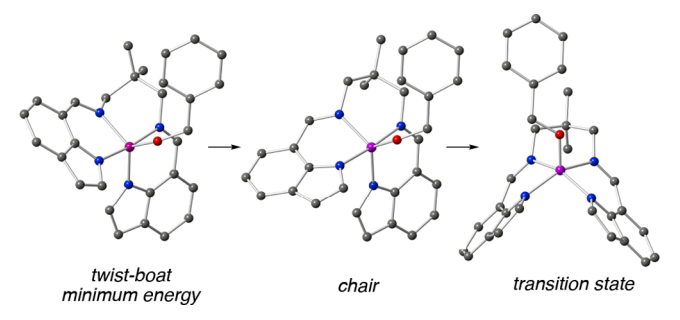


Figure 4. Calculated structures for the fluxional process that interconverts Δ and Λ enantiomers of L^7AlOBn , depicting the lowest energy structure for the Δ enantiomer, the next highest energy (+ 2.3 kcal mol $^{-1}$) structure for the chair conformation of the metallacycle, and the "symmetric" transition state structure.

L²AlOBn, the metallacycle is already in a chair-like conformation, so the chirality flipping happens in one step (Figure S43). Finally, we note parenthetically that the catalyst fluxionality for these systems resembles that proposed for Ti complexes that catalyze syndiospecific propene polymerization.⁹

Polymerization Behavior. We examined the catalytic polymerization of rac-LA by L⁷AlOBn and L²AlOBn under a variety of conditions, ranging from 35 °C in CD₂Cl₂ (300:1 monomer:catalyst ratio, except in the case of toluene) to neat reactions in the melt (135–180 °C). As indicated in Table 1, the reactions proceeded at rates that depended on the conditions used to yield PLA characterized by low \mathcal{D} values (measured by size exclusion chromatography using light scattering detection) and P_m values (measured via analysis of homonuclear decoupled ¹H NMR data, examples in Figures S17-S19 and Table S2). These latter values varied from 0.53 (low isotacticity, entries 9 and 14) to 0.80 (high isotacticity, entries 1 and 2), depending on the supporting ligand and the conditions. The results for polymerizations by L²AlOBn are similar to those reported recently. Differential scanning calorimetry data revealed $T_{\rm m}$ features in only three cases (entries 1-3, Table 1, examples shown in Figures S20-S23), indicating attainment of isotactic segment lengths sufficient for crystallization in these instances. Previously reported data for (TBSsalen)AlOR⁴ⁿ are shown for comparison (entries 15, 17, 19, Table 1), along with data for the same complex that we prepared and tested independently (entries 16, 18, 20, Table 1) that are in good agreement. In general, the level of stereocontrol exhibited by (TBSsalen)AlOR was higher than for L⁷AlOBn and L²AlOBn. The stereoselectivity exhibited by the complex of $(L^7)^{2-}$ is slightly higher than that supported by $(L^2)^{2-}$, which exhibits faster rates than the former.

Experimental Insights into Stereocontrol in Initiation. In order to begin to understand the basis for stereocontrol for *rac*-LA polymerization by L^7 AlOBn and L^2 AlOBn, we examined stoichiometric reactions of *rac*-, L(S,S)-, and D(R,R)-LA with the complexes, as well as with (TBSsalen)AlOBn for comparison. In the experiments, a

Table 1. Data for Polymerizations of rac-LA by the Indicated Complexes

entry	complex	temp. (°C)	LA:cat	time	convn ^a (%)	$M_{\rm n}~({ m kDa})^{b}$	D^b	$P_{\mathrm{m}}^{}c}$	$T_{\rm m} ({}^{\circ}{\rm C})^d$
1	L ⁷ AlOBn	35 (CD ₂ Cl ₂)	300	14 d	99	85	1.06	0.80	163
2		55 (THF-d ₈)	300	4 d	99	36	1.03	0.80	155
3		70 (tol-d ₈)	100	3 d	98	24	1.20	0.74	150
4		135	300	30 min	96	40	1.11	0.64	e
5		150	300	25 min	78	85	1.22	0.63	e
6		165	300	20 min	91	29	1.16	0.66	e
7		180	300	15 min	93	54	1.44	0.68	e
8	L^2AlOBn	35 (CD ₂ Cl ₂)	300	6 d	95	35	1.08	0.67	e
9		55 (THF-d ₈)	300	2 d	99	42	1.17	0.53	e
10		70 (tol-d ₈)	100	3 d	98	24	1.31	0.67	e
11		135	300	30 min	93	34	1.74	0.58	e
12		150	300	25 min	94	60	1.85	0.62	e
13		165	300	20 min	79	115	1.31	0.55	e
14		180	300	15 min	99	64	1.23	0.53	e
15	(TBSsalen)AlOR ^g	70 (tol-d ₈)	100	14 h	96	22^f	1.07 ^f	0.98	209
16					96	25	1.07	0.92	207
17		130	300	30 min	73	44 ^f	1.08^{f}	0.92	189
18					79	53	1.15	0.89	187
19		180	300	20 min	91	60 ^f	1.13^{f}	0.84	176
20		L			90	59	1.34	0.85	179

"Determined by ¹H NMR spectroscopy. Except as noted, these values were determined by SEC using light scattering detection with THF eluent. Theoretical values are 44 kDa for 300 equiv of LA and 15 kDa for 100 equiv of LA. Determined by homonuclear decoupled ¹H NMR spectroscopy (see SI). Determined by DSC. No feature corresponding to a $T_{\rm m}$ value was observed. Values determined by SEC using a refranctive index detector and polystyrene standards with CHCl₃ eluent. Previously reported values (ref 4n with values we independently determined below in italics).

solution of LA (1 equiv) in CD₂Cl₂ or CDCl₃ was added to a solution of the complex in the same solvent (6.5 mM) at room temperature and a ¹H NMR spectrum was immediately measured. The spectra showed complete consumption of starting materials and the appearance of predominantly one species with new peaks that we assign to the single ring-opened products L²- or L⁷Al(oLAOBn) (where oLAOBn refers to the ring-opened LA terminated by -OBn; Figures 5, S5-S8) or (TBSsalen)Al(oLAOBn) (Figures S9 and S10), as reported previously. 4n Importantly, the spectra for the products of the reactions with *rac*-, L(S,S)-, and D(R,R)-LA are nearly identical. The peak patterns are consistent with selective formation of either a 1:1 mixture of two symmetric complexes (i.e., indolide or phenolate rings are equivalent for each, which would only be possible if peaks due to diastereomeric species were averaged as a result of fluxionality) or a single asymmetric complex (with inequivalent rings). Thus, for example, the spectra of L⁷Al(oLAOBn) exhibit two peaks (8.37 and 8.45 ppm) integrating equally for the imine protons; these peaks are almost overlapping for the case of L²Al(oLAOBn).

To interpret the results from NMR spectroscopy, we present all the possible structures for the products of ring-opening of D(R,R)- and L(S,S)-LA by the two interconverting stereo-isomers of L^7 AlOBn in Scheme 2. Thus, each stereoisomer Δ - or Λ - L^7 AlOBn can react with either L(S,S)-LA or D(R,R)-LA. The result is four possible stereoisomers, classified as two diastereomeric pairs of enantiomers: Δ - $L(S,S)/\Lambda$ -D(R,R) and Δ - $D(R,R)/\Lambda$ -L(S,S). These are drawn with the opened LA chain binding in bidentate fashion via alkoxide and carbonyl O atoms, which is what we observed via X-ray crystallography (vide infra). Each pair of enantiomers (i.e., each diastereomeric set) would be expected to give rise to a spectrum featuring inequivalent indolide rings and one set of peaks associated with the opened LA chain. The observed spectrum for the reaction

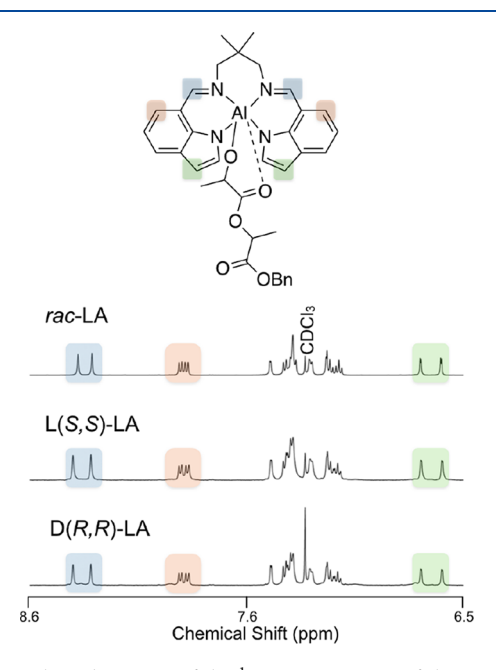


Figure 5. Selected portion of the 1 H NMR spectra of the products of the reactions of (top) *rac*-LA, (middle) $_L(S,S)$ -LA, or (bottom) $_D(R,R)$ -LA with $_L^7$ AlOBn, with the indicated assignments. Full spectra as well as data for the same reactions of $_L^2$ AlOBn are provided as Figures S5–S8.

with *rac*-LA (e.g., the pairs of peaks of equal intensity shown in Figure 5) is consistent with highly stereoselective formation of *one* of the diastereomeric sets (i.e., one pair of enantiomers). The observation of the same spectrum in reactions of pure L(S,S)- or D(S,S)-LA is explained by selective formation of one diastereomer (i.e., for the reaction with L(S,S)-LA, either Δ -L(S,S) or Δ -L(S,S). The NMR data are not sufficient to

Scheme 2. Possible Products L⁷Al(oLAOBn) Resulting from the Reaction of the Interconverting Stereoisomers L⁷AlOBn (in box) with L(S,S)- and D(R,R)-LA, Labeled According to the Configuration at Al (Δ vs. Λ) and LA (D(R,R) vs. L(S,S))^a

"The isomers labeled "X-ray" are the ones identified by X-ray crystallography.

distinguish which set of enantiomers (for the reaction with *rac*-LA) or which particular diastereomer (for the reactions with pure L(S,S)- or D(R,R)-LA) is formed. The alternative explanation that the peaks observed are due to a rapidly interconverting mixture of *both* diastereomers would predict line broadening or decoalescence of these peaks upon lowering the temperature, but this was not observed (to $-88\,^{\circ}$ C, Figures S12 and S14). Finally, we note that similar considerations apply to the (TBSsalen)Al system.

By layering pentane on CD_2Cl_2 solutions of the products L^2 -or $L^7Al(oLAOBn)$ formed upon reaction of L^2AlOBn and L^7AlOBn with rac-LA and storing at -30 °C, we obtained crystals suitable for X-ray diffraction (Figure 6). In both cases, the ring-opened products crystallized as a pair of enantiomers comprising a *single* diastereomer, consistent with our interpretation of the ¹H NMR spectra of the product solutions. These enantiomers were identified as the complexes labeled Δ -L(S,S) and Λ -D(R,R) in Scheme 2, with only the former enantiomer for each case shown in Figure 6. In both structures (a and b), the Al-O1 (alkoxide) distance (1.804(2) Å and 1.807(3) Å, respectively) is shorter than all other metal-ligand

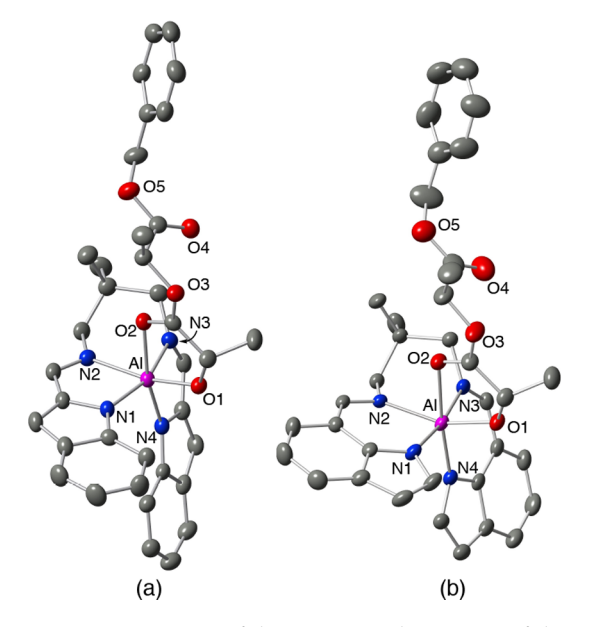


Figure 6. Representations of the X-ray crystal structures of the ringopened products (a) L²Al(oLAOBn) and (b) L⁷Al(oLAOBn), resulting from the reactions of L²AlOBn and L⁷AlOBn, respectively, with 1 equiv of rac-LA. Only a single enantiomer for each structure is shown $(\Delta-L(S,S))$; the other $\Lambda-D(R,R)$ enantiomer is also present in the unit cell), with all atoms presented as 50% ellipsoids and hydrogen atoms omitted for clarity. Selected bond distances (Å) and angles (deg): (a) Al1–O1, 1.804(2); Al1–N1, 1.932(3); Al1–N2, 2.058(5); Al1-N3, 2.054(1); Al1-N4, 1.945(0); N3-Al1-N1, 160.070(6); N3-Al1-O1, 99.876(5); N3-Al1-O2, 88.536(1); N3-Al1-N2, 79.984(0); N3-Al1-N4, 80.830(1); N2-Al1-N4, 100.140(0); O2-Al1-O1, 81.204(6); N2-Al1-O2, 84.416(7); N4-Al1-O1, 94.002(8); N4-Al1-O2, 167.451(7); N1-Al1-N4, 102.280(5), N1-Al1-N2, 80.091(8); N1-Al1-O2, 89.986(1); N1-Al1-O1, 99.531(4); (b) Al1-O1, 1.807(3); Al1-N1, 1.9475(18); Al1-N2, 2.0647(16); Al1-N3, 2.0779(18); Al1-N4, 1.9344(17); N3-Al-N1, 171.24(7); N3-Al1-O1, 90.80(8); N3-Al1-O2, 89.33(13); N3-Al1-N2, 82.69(6); N3-Al1-N4, 89.49(7); N2-Al1-N4, 103.71(7); O2-Al1-O1, 79.47(11); N2-Al1-O2, 81.07(9); N4-Al1-O1, 95.56(9); N4-Al1-O2, 174.88(12); N1-Al1-N4, 94.99(7); N1-Al1-N2, 88.93(7); N1-Al1-O2, 86.84(14); N1-Al1-O1, 96.24(9).

bonds (range 2.094(7)-1.932(3) Å). The Al geometries are octahedral, with the ring-opened LA bound in bidentate fashion featuring Al-O2 distances of 2.094(7) Å and 2.1784(17) Å for (a) and (b), respectively. These X-ray structures represent rare examples of high quality structural determinations for ring-opened LA bound to a metal complex. Such species had been previously identified by spectroscopy 4h,j,k,13 and modeled in structures of methyl lactate complexes.

Redissolution of the crystals used for the X-ray structure determinations yielded ^{1}H NMR spectra identical to those obtained for the initial product solutions. These results are consistent with the NMR spectral features arising from the Δ -L(S,S) and Λ -D(R,R) enantiomers (the single diastereomer) observed by X-ray crystallography. Nonetheless, it is also possible that the diastereomer observed by NMR spectroscopy participates in an equilibrium with a small (essentially unobservable) amount of the other diastereomer (vide infra), and that this minor diastereomer preferentially crystallizes (and reverts to the major diastereomer upon redissolution). While we view this alternative possibility as unlikely (preferential

crystallization of an equilibrating minor diastereomer for both $(L^2)^{2-}$ and $(L^7)^{2-}$ systems), it cannot be ruled out by the available experimental data.

The above considerations raise the question: Is the initiation reaction selectivity based on kinetic or thermodynamic control? That is, does the initiation stereoselectivity result from differences in the barriers for ring-opening (as postulated previously on the basis of theory for other catalysts) or from differences in the stabilities of the products that are rapidly equilibrating? Such equilibration might involve rapid intermolecular exchange of alkoxide ligands (e.g., between Δ -L(S,S) and Δ -D(R,R) isomers), decoordination of the carbonyl group and racemization at Al as observed for the fluxionality of LAlOBn (e.g., between Δ -L(S,S) and Λ -L(S,S) isomers), or both (Figure 7).

OBN OODN
$$X$$
-ray X -

Figure 7. Illustration of possible interconversions of stereoisomers $L^7Al(oLAOBn)$. The red arrows indicate processes involving intermolecular exchange of LA enantiomers, blue arrows correspond to racemization at Al (e.g., via carbonyl decoordination, isomerization, and recoordination), and black arrows correspond to both.

To test for these possibilities, we performed a set of experiments using NMR exchange spectroscopy (EXSY).¹⁶ The experiments involved acquisition of data on solutions of (a) L⁷Al(oLAOBn) and L²Al(oLAOBn) prepared from reactions of the respective benzyloxide complexes with rac-LA, (b) L⁷Al(oLAOBn) prepared from reaction of L⁷AlOBn with L(S,S)-LA, (c) a 1:1 mixture of L^7 Al(oLAOBn) and L²Al(oLAOBn) prepared by mixing solutions resulting from reaction of the respective benzyloxide complexes with rac-LA, and (d) a 1:1 mixture of L⁷Al(oLAOBn) and (TBSsalen)-AlOBn prepared by mixing solutions resulting from reaction of the respective benzyloxide complexes with rac-LA. The results and detailed interpretations are described in the Supporting Information (Figures S28-S34); here, we present the primary conclusions drawn. From part a, we identified minor peaks in the NMR spectra that we assign to small amounts of the minor diastereomer, and clear evidence of exchange between the ring-

opened alkoxide chains indicating interconversion between the major and minor diastereomers. By integration, the ratio (K_{eq}) of the equilibrating major:minor isomers for L⁷Al(oLAOBn) is ~ 9:1, corresponding to $\Delta G^{\circ}_{298} = -1.3 \text{ kcal mol}^{-1}$. Using EXSYcalc, ¹⁷ rate constants of 4.1 s⁻¹ and 0.44 s⁻¹ were obtained, which correspond to $K_{\rm eq} \sim 9$, in good agreement with the integration ratio. Similarly, for L²Al(oLAOBn), K_{eq} by integration is ~ 9.5 and $\Delta G^{\circ}_{298} = -1.3$ kcal mol⁻¹, with rate constants 2.2 s⁻¹ and 0.25 s⁻¹, giving $K_{\rm eq} \sim 8.8$. From part b, wherein only one enantiomer of LA was used, the data indicated that racemization at Al occurred. From parts c and d, exchange between peaks of the mixed complexes indicated the occurrence of intermolecular swapping of alkoxide chains. Taken together, the EXSY data are consistent with rapid equilibria in solution among all species (illustrated in Figure 7 for the case of L7Al(oLAOBn)), favoring one diastereoisomeric pair ($K_{eq} = 9$), via all possible pathways (intermolecular alkoxide exchange and racemization at Al). Importantly, the data support thermodynamic control of stereoselectivity in the initiation, such that the product ratio is controlled by the relative stability of the products that rapidly equilibrate.

Theory. To better understand factors contributing to stereocontrol in the initiation process that we were able to characterize experimentally, the free energy profiles for the initiation steps associated with both L²AlOR and L⁷AlOR were computationally determined for both L(S,S)- and D(R,R)-LA (see Supporting Information for details). Both L⁷AlOMe and L⁷AlOBn were examined in order to assess the significance of variation of the alkoxide. Since the results were similar, only the methoxy initiator was considered for all other catalysts in order to reduce computational cost.

For initiation, three structural descriptors define all possible pathways. These are (i) the LA coordination mode, (ii) the chirality of the LA monomer, and (iii) the prochirality of the LA carbonyl group subject to nucleophilic attack. The calculated pathway for all systems is illustrated for one particular catalyst enantiomer (Δ -L²AlOMe), one substrate enantiomer (D(R,R)-LA), and one particular approach trajectory (prochirality; see below) in Figure 8. The process

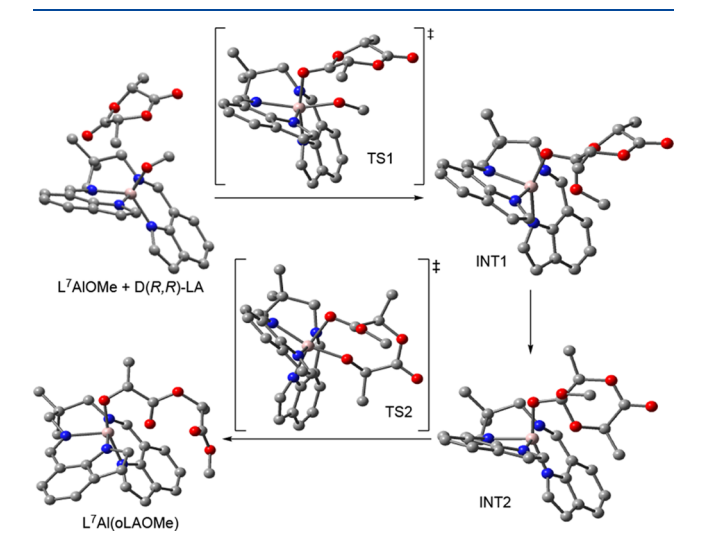


Figure 8. Illustration of the calculated initiation pathway for a selected catalyst (Δ -L⁷AlOMe), substrate (D(R,R)-LA), and approach trajectory. H atoms are not shown for clarity. Key: pink = Al, red = O, blue = N, and gray = C.

involves LA binding and attack of the alkoxy group at the LA carbonyl via TS1 to yield INT1. After rearrangement to INT2 (which involves shifting which ether oxygen of the tetrahedral intermediate is bound to the metal), ring-opening via TS2 yields the product comprising one incorporated LA unit. While we find no minima where LA coordinates to aluminum prior to nucleophilic attack—instead, only van der Waals complexes with long Al-O distances exist on the potential energy surface—coordination is present in transition-state (TS1) structures for nucleophilic attack, and there are two possibilities for the relative position of the LA monomer: trans either to the N atom of an indole or to the N atom of a backbone imine (each alternative then dictates the position of the alkoxy group). The LA itself may be D(R,R) or L(S,S), and finally the re or si prochirality of the face of the LA carbonyl group exposed to the alkoxy ligand sets the rotational degree of freedom for the monomer. Given these differentiating structural factors, there are a total of 8 pathways that must be considered in order to comprehensively assess all possible initiation paths for a given catalyst enantiomer (Figure 9).

Figure 9. Starting structures along the eight alternative pathways for initiation of D(R,R)- and L(S,S)-LA for Δ -L⁷AlOMe. The cis and trans descriptors indicate the positions of the imine groups of the complex with respect to the LA, specifically, in the trans pathway, the LA C= O is trans to *one* imine group while in the cis pathway it is cis to *both* imine groups.

The results of energetic calculations for all reaction pathways involving Δ -L⁷AlOMe, -L⁷AlOBn, and -L²AlOMe are shown in Table 2; data for (TBSsalen)AlOMe are shown in Table S8. Where shown, product energies are listed for two pathways; all other pathways lead to one of those products. Finally, overall barriers for initiation are shown in the last column. A more detailed discussion of the structural factors leading to the

Table 2. Free Energies (kcal mol⁻¹) for Stationary Points along the Various Reaction Pathways for Initiation of LA by Δ -L⁷AlOMe, Δ -L⁷AlOBn, and Δ -L²AlOMe^a

path	TS1	INT1	INT2	TS2	prod	tot.b							
L^7 AlOMe													
cis-D-si	9.8	2.7	3.7	14.7	-14.8	14.7							
cis-D-re	8.8	-0.5	3.0	8.4	11.0	8.9							
cis-L-re	9.0	1.5	4.8	11.0	-15.9	11.0							
cis-L-si	8.7	0.5	3.6	11.3	1017	11.3							
trans-D-si	11.6	4.8	3.8	20.2		20.2							
trans-D-re	8.5	1.7	2.3	7.8		8.5							
trans-L-re	9.7	3.3	5.5	11.8		11.8							
trans-L-si	10.8	2.1	4.3	14.7		14.7							
$L^{7}AlOBn$													
cis-D-si	9.4	3.6	5.3	17.5		17.5							
cis-D-re	11.9	3.7	4.9	10.7		11.9							
cis-L-re	9.4	3.4	6.2	13.8		13.8							
cis-L-rc	10.3	3.1	3.8	12.7		12.7							
trans-D-si	19.0	12.2	11.6	28.9		28.9							
trans-D-si	17.4	10.6	10.2	15.7		17.4							
trans-L-re	16.4	12.0	13.5	19.3		19.3							
trans-L-si	19.3	13.4	13.6	23.9		23.9							
truns-L-st	19.3		² AlOMe	23.9		23.9							
cis-D-si	9.5	4.8	4.8	21.1	-9.9	21.1							
cis-D-si	7.3	0.8	4.7	8.4	-9.9	8.4							
cis-L-re	8.0	2.4	5.2	9.6	-10.4	9.6							
					-10.4								
cis-L-si	10.0	2.4	9.7	12.6		12.6							
trans-D-si	14.9	6.9	6.4	51.5		51.5							
trans-D-re	9.4	2.0	3.8	10.7		10.7							
trans-L-re	10.4	4.0	6.2	12.5		12.5							

"Gibbs free energies (kcal mol $^{-1}$, 298.15 K) computed at SMD/M06-2X/6-311+G(d,p)//M06-L/6-31+G(d,p) level for stationary points. Lowest total energies for catalyst indicated in bold. b Tot. = overall energy barrier.

energetic ordering observed in Tables 2 and S7 is found in the Supporting Information. Comparing the results in these tables, it is apparent that for both methoxy and benzyloxy as an initiator, reaction of the Δ isomer of the complexes with D(R,R)-LA is calculated to be kinetically favored for all complexes. There are differences in whether the cis-re or transre pathways are preferred, depending on the nature of the ligands (see Supporting Information). Importantly, these findings for the kinetic preferences are in disagreement with the stereochemistry observed in the X-ray crystal structures of L²Al(oLAOBn) and L⁷Al(oLAOBn) (Figure 6). In contrast, the Δ -L(S,S) isomer observed by X-ray crystallography is calculated to be thermodynamically more favorable for both L⁷AlOMe and, to a lesser extent, L²AlOMe. While the computed energy differences are small, suggesting that product mixtures might be expected under thermodynamic conditions, the agreement with the $\Delta G^{\circ}_{298} = -1.3 \text{ kcal mol}^{-1}$ for the postulated equilibria between the diastereomers determined from integration of NMR spectra is reasonable considering the inherent accuracy of the calculations (ca. ± 1 kcal mol⁻¹). Thus, the computations corroborate the conclusions drawn experimentally, that the stereoselectivity observed is determined by the relative thermodynamic stability of the products, and that the preferred stereoisomer is that which was characterized structurally by X-ray crystallography. Again, however, because the calculated energy differences between

the products are small, we cannot unambiguously rule out the possibility that the minor isomer is the one that crystallizes.

Putting these findings in context, previous DFT investigations of the origins of stereoselectivity in LA polymerizations by metal-alkoxide catalysts have focused on differences in kinetic barriers for ring-opening of LA stereoisomers. 15,18-21 Both kinetic and thermodynamic preferences were identified by theory for the addition of a second monomer to the initially formed ring-opened species in syndiotactic polymerization of rac-β-butyrolactone by yttrium catalysts supported by salantype ligands.²² Small energetic differences arising from subtle secondary interactions (typically with the growing chain end in propagation steps) were identified in the previous DFT studies.²³ While general rules for predicting stereoselectivity are lacking, the finding herein that thermodynamic control of stereoselectivity in ROTEP initiation suggests that similar ideas should be considered in evaluating stereocontrol in propagation reactions.

SUMMARY AND CONCLUSIONS

We have synthesized and characterized the solution and solid state structures of the complexes L²AlOBn and L⁷AlOBn, including the delineation of the nature of the fluxional process that interconverts the enantiomeric forms of the complexes through VT-NMR spectroscopy and computations. The complexes polymerize rac-LA stereoselectively. As a first step toward developing a molecular-level understanding of the mechanistic basis for the observed stereoselectivity, we studied the initiation reaction. Treatment of the complexes with 1 equiv of rac-LA yielded the ring-opened products L²Al-(oLAOBn) and L⁷Al(oLAOBn), and on the basis of NMR spectroscopy, the major product for each reaction was identified as a single diastereomer (pair of enantiomers). Crystals isolated from the product solutions were characterized by X-ray diffraction, revealing unambiguously for the first time the detailed molecular structure and stereochemistry of a product of initiation of cyclic ester polymerization by a metalalkoxide complex. Studies of the product solutions by EXSY NMR showed that the products exist as stereoisomers that rapidly interconvert via both intermolecular alkoxide exchange and racemization at the Al center. Examination of the initiation reactions by theory delineated the mechanistic details, in particular the reaction energetics as a function of stereochemistry. We conclude, with appropriate caveats because of the small energetic differences found by theory, that the stereoselectivity observed in the initiation reaction is likely not the result of kinetic preferences (which predict preferential formation of the stereoisomer not observed by X-ray crystallography). Instead, thermodynamic control of selectivity is supported by the experimental NMR data indicative of equilibration of diastereomers in solution and by the prediction by theory that the stereoisomer observed by X-ray crystallography is the most stable (keeping in mind the possibility, albeit in our view unlikely, that the crystals isolated could be the minor isomer).

In addition to providing specific information on particular systems, the mechanistic results reported herein significantly augment our general understanding of stereocontrol of ROTEP initiation by metal-alkoxide complexes and suggest the importance of thermodynamic control in determining the favored product stereoisomer. We speculate that similar considerations apply to understanding subsequent monomer enchainment, the stereochemistry of which may similarly rely

on product stability rather than kinetic barriers typically emphasized in theoretical studies.

ASSOCIATED CONTENT

Supporting Information

The Supporting Information is available free of charge at https://pubs.acs.org/doi/10.1021/acs.macromol.0c00092.

Experimental and computational details and spectra (PDF)

Cartesian coordinates (ZIP)

AUTHOR INFORMATION

Corresponding Authors

Christopher J. Cramer — Department of Chemistry, NSF Center for Sustainable Polymers, and Supercomputing Institute, University of Minnesota, Minneapolis, Minnesota 55455, United States; Occid.org/0000-0001-5048-1859; Email: cramer@umn.edu

Theresa M. Reineke — Department of Chemistry and NSF Center for Sustainable Polymers, University of Minnesota, Minneapolis, Minnesota 55455, United States; orcid.org/0000-0001-7020-3450; Email: treineke@umn.edu

William B. Tolman – Department of Chemistry and NSF Center for Sustainable Polymers, Washington University in St. Louis, St. Louis, Missouri 63130, United States; orcid.org/ 0000-0002-2243-6409; Email: wbtolman@wustl.edu

Authors

Anna M. Luke — Department of Chemistry and NSF Center for Sustainable Polymers, University of Minnesota, Minneapolis, Minnesota 55455, United States; orcid.org/0000-0001-9486-5635

Appie Peterson — Department of Chemistry and NSF Center for Sustainable Polymers, Washington University in St. Louis, St. Louis, Missouri 63130, United States; orcid.org/0000-0002-2824-7545

Sina Chiniforoush — Department of Chemistry, NSF Center for Sustainable Polymers, and Supercomputing Institute, University of Minnesota, Minneapolis, Minnesota 55455, United States; orcid.org/0000-0002-8428-4228

Mukunda Mandal — Department of Chemistry, NSF Center for Sustainable Polymers, and Supercomputing Institute, University of Minnesota, Minneapolis, Minnesota 55455, United States; orcid.org/0000-0002-5984-465X

Yanay Popowski — Department of Chemistry and NSF Center for Sustainable Polymers, Washington University in St. Louis, St. Louis, Missouri 63130, United States; orcid.org/0000-0003-1569-0035

Hussnain Sajjad — Department of Chemistry, University of Minnesota, Minneapolis, Minnesota 55455, United States; orcid.org/0000-0003-1283-5884

Caitlin J. Bouchey — Department of Chemistry, Washington University in St. Louis, St. Louis, Missouri 63130, United States; Occid.org/0000-0003-0729-6839

Dimitar Y. Shopov — Department of Chemistry, Washington University in St. Louis, St. Louis, Missouri 63130, United States; orcid.org/0000-0002-4689-4383

Brendan J. Graziano — Department of Chemistry, University of Minnesota, Minneapolis, Minnesota 55455, United States;
occid.org/0000-0003-1449-9255

Letitia J. Yao — Department of Chemistry, University of Minnesota, Minneapolis, Minnesota 55455, United States; orcid.org/0000-0001-9945-558X

Complete contact information is available at: https://pubs.acs.org/10.1021/acs.macromol.0c00092

Author Contributions

§A.M.L. and A.P. contributed equally to the research.

The authors declare no competing financial interest.

ACKNOWLEDGMENTS

This work was supported by the NSF Center for Sustainable Polymers, a NSF Center for Chemical Innovation, CHE-1901635. X-ray diffraction data were collected using diffractometers acquired through NSF-MRI Award No. CHE-1229400 (University of Minnesota) or 1827756 (Washington University in St. Louis).

REFERENCES

- (1) Selected lead references: (a) Schneiderman, D. K.; Hillmyer, M. A. 50th Anniversary Perspective: There Is a Great Future in Sustainable Polymers. *Macromolecules* **2017**, *50*, 3733–3749. (b) Wu, J. C.; Yu, T. L.; Chen, C. T.; Lin, C. C. Recent developments in main group metal complexes catalyzed/initiated polymerization of lactides and related cyclic esters. *Coord. Chem. Rev.* **2006**, *250*, 602–626. (c) Coates, G. W.; Moore, D. R. Discrete Metal-Based Catalysts for the Copolymerization of CO₂ and Epoxides: Discovery, Reactivity, Optimization, and Mechanism. *Angew. Chem., Int. Ed.* **2004**, *43*, 6618–6639. (d) Dechy-Cabaret, O.; Martin-Vaca, B.; Bourissou, D. Controlled Ring-Opening Polymerization of Lactide and Glycolide. *Chem. Rev.* **2004**, *104*, 6147–6176.
- (2) Stanford, M. J.; Dove, A. P. Stereocontrolled ring-opening polymerisation of lactide. *Chem. Soc. Rev.* **2010**, 39, 486–494.
- (3) Drumright, R. W.; Gruber, P. R.; Henton, D. E. Polylactic Acid Technology. *Adv. Mater.* **2000**, *12*, 1841–1846. Uhrich, K. E.; Cannizzaro, S. M.; Langer, R. S.; Shakesheff, K. M. Polymeric Systems for Controlled Drug Release. *Chem. Rev.* **1999**, *99*, 3181–3198.
- (4) Le Borgne, A.; Vincens, V.; Jouglard, M.; Spassky, N. Ringopening oligomerization reactions using aluminium complexes of Schiff's bases as initiators. Makromol. Chem., Macromol. Symp. 1993, 73, 37-46. (b) Spassky, N.; Wisniewski, M.; Pluta, C.; Le Borgne, A. Highly Stereoelective Polymerization of Rac-(D,L)-Lactide with a Chiral Schiff's base/Aluminium Alkoxide Initator. Macromol. Chem. Phys. 1996, 197, 2627-2637. (c) Wisniewski, M.; Borgne, A. L.; Spassky, N. Synthesis and properties of (D)- and (L)-lactide stereocopolymers using the system achiral Schiff's base/aluminium methoxide as initiator. Macromol. Chem. Phys. 1997, 198, 1227-1238. (d) Ovitt, T. M.; Coates, G. W. Stereoselective Ring-Opening Polymerization of meso-Lactide: Synthesis of Syndiotactic Poly(lactic acid). J. Am. Chem. Soc. 1999, 121, 4072-4073. (e) Radano, C. P.; Baker, G. L.; Smith, M. R., III Stereoselective Polymerization of a Racemic Monomer with a Racemic Catalyst: Direct Preparation of the Polylactic Acid Stereocomplex from Racemic Lactic Acid. J. Am. Chem. Soc. 2000, 122, 1552-1553. (f) Ovitt, T. M.; Coates, G. W. Stereoselective ring-opening polymerization of rac-lactide with a single-site, racemic aluminum alkoxide catalyst: Synthesis of stereoblock poly(lactic acid). J. Polym. Sci., Part A: Polym. Chem. 2000, 38, 4686-4692. (g) Majerska, K.; Duda, A. Stereocontrolled Polymerization of Racemic Lactide with Chiral Initiator: Combining Stereoelection and Chiral Ligand-Exchange Mechanism. J. Am. Chem. Soc. 2004, 126, 1026-1027. (h) Chisholm, M. H.; Patmore, N. J.; Zhou, Z. Concerning the relative importance of enantiomorphic site vs. chain end control in the stereoselective polymerization of lactides: reactions of (R,R-salen)- and (S,S-salen)-aluminium alkoxides LAlOCH2R complexes (R = CH3 and S-CHMeCl).
- Chem. Commun. 2005, 127-129. (i) Zhong, Z.; Dijkstra, P. J.; Feijen, J. [(salen)Al]-Mediated, Controlled and Stereoselective Ring-Opening Polymerization of Lactide in Solution and without Solvent: Synthesis of Highly Isotactic Polylactide Stereocopolymers from Racemic D,L.-Lactide. Angew. Chem., Int. Ed. 2002, 41, 4510-4513. (j) Zhong, Z.; Dijkstra, P. J.; Feijen, J. Controlled and Stereoselective Polymerization of Lactide: Kinetics, Selectivity, and Microstructures. J. Am. Chem. Soc. 2003, 125, 11291-11298. (k) Chisholm, M. H.; Gallucci, J. C.; Quisenberry, K. T.; Zhou, Z. Complexities in the Ring-Opening Polymerization of Lactide by Chiral Salen Aluminum Initiators. Inorg. Chem. 2008, 47, 2613-2624. (1) Nomura, N.; Ishii, R.; Akakura, M.; Aoi, K. Steroselective Ring-Opening Polymerization of Racemic Lactide Using Aluminum-Achiral Ligand Complexes: Exploration of a Chain-End Control Mechanism. J. Am. Chem. Soc. 2002, 124, 5938-5939. (m) Hormnirun, P.; Marshall, E. L.; Gibson, V. C.; White, A. J. P.; Williams, D. J. Remarkable Stereocontrol in the Polymerization of Racemic Lactide Using Aluminum Initiators Supported by Tetradentate Aminophenoxide Ligands. J. Am. Chem. Soc. 2004, 126, 2688-2689. (n) Nomura, N.; Ishii, R.; Yamamoto, Y.; Kondo, T. Stereoselective Ring-Opening Polymerization of a Racemic Lactide by Using Achiral Salen- and Homosalen-Aluminum Complexes. Chem. - Eur. J. 2007, 13, 4433-4451. (o) Hormnirun, P.; Marshall, E. L.; Gibson, V. C.; Pugh, R. I.; White, A. J. P. Polymerization Special Feature: Study of ligand substituent effects on the rate and stereoselectivity of lactide polymerization using aluminum salen-type initiators. Proc. Natl. Acad. Sci. U. S. A. 2006, 103, 15343-15348. (p) Tang, Z.; Chen, X.; Pang, X.; Yang, Y.; Zhang, X.; Jing, X. Stereoselective Polymerization of rac-Lactide Using a Monoethylaluminum Schiff Base Complex. Biomacromolecules 2004, 5, 965-970. (q) Alaaeddine, A.; Thomas, C. M.; Roisnel, T.; Carpentier, J.-F. Aluminum and Yttrium Complexes of an Unsymmetrical Mixed Fluorous Alkoxy/Phenoxy-Diimino Ligand: Synthesis, Structure, and Ring-Opening Polymerization Catalysis. Organometallics 2009, 28, 1469-1475.
- (5) Mandal, M.; Luke, A. M.; Dereli, B.; Elwell, C. E.; Reineke, T. M.; Tolman, W. B.; Cramer, C. J. Computational Prediction and Experimental Verification of ε -Caprolactone Ring-Opening Polymerization Activity by an Aluminum Complex of an Indolide/Schiff-Base Ligand. *ACS Catal.* **2019**, *9*, 885–889.
- (6) Du, H.; Velders, A. H.; Dijkstra, P. J.; Zhong, Z.; Chen, X.; Feijen, J. Polymerization of Lactide Using Achiral Bis(pyrrolidene) Schiff Base Aluminum Complexes. *Macromolecules* **2009**, 42, 1058–1066.
- (7) Wei, Y.; Song, L.; Jiang, L.; Huang, Z.; Wang, S.; Yuan, Q.; Mu, X.; Zhu, X.; Zhou, S. Aluminum complexes with Schiff base bridged bis(indolyl) ligands: synthesis, structure, and catalytic activity for polymerization of rac-lactide. *Dalton Trans* **2019**, *48*, 15290–15299.
- (8) Addison, A. W.; Rao, T. N.; Reedijk, J.; van Rijn, J.; Verschoor, G. C. Synthesis, structure, and spectroscopic properties of copper(II) compounds containing nitrogen—sulphur donor ligands; the crystal and molecular structure of aqua[1,7-bis(N-methylbenzimidazol-2'-yl)-2,6-dithiaheptane]copper(II) perchlorate. *J. Chem. Soc., Dalton Trans.* 1984, 1349—1356.
- (9) (a) Tian, J.; Hustad, P. D.; Coates, G. W. A New Catalyst for Highly Syndiospecific Living Olefin Polymerization: Homopolymers and Block Copolymers from Ethylene and Propylene. *J. Am. Chem. Soc.* **2001**, *123*, 5134–5135. (b) Milano, G.; Cavallo, L.; Guerra, G. Site Chirality as a Messenger in Chain-End Stereocontrolled Propene Polymerization. *J. Am. Chem. Soc.* **2002**, *124*, 13368–13369.
- (10) As expected, comparison of the kinetics of polymerizations of L-LA and rac-LA by both L^7 AlOBn and L^2 AlOBn showed a higher rate for the single enantiomer (i.e., L-LA; Figure S4).
- (11) While the imine peaks were not perturbed upon lowering the temperature, significant changes in the peaks arising from the ring-opened LA chain were seen (Figures S12 and S14). We speculate that these may arise from changes in the chain conformations, but do not have further unambiguous insights, in part due to the complexity of the chain structures. We also note that the alternative explanation for

ı

the two imine peaks (averaging of peaks due to both diastereomers) is inconsistent with the EXSY data discussed later in the text.

- (12) (a) Dagorne, S.; Le Bideau, F.; Welter, R.; Bellemin-Laponnaz, S.; Maisse-François, A. Well-Defined Cationic Alkyl— and Alkoxide—Aluminum Complexes and Their Reactivity with ε -Caprolactone and Lactides. *Chem. Eur. J.* **2007**, *13*, 3202—3217. (b) Lewiński, J.; Horeglad, P.; Wójcik, K.; Justyniak, I. Chelation Effect in Polymerization of Cyclic Esters by Metal Alkoxides: Structure Characterization of the Intermediate Formed by Primary Insertion of Lactide into the Al—OR Bond of an Organometallic Initiator. *Organometallics* **2005**, *24*, 4588—4593.
- (13) Trofimoff, L.; Aida, T.; Inoue, S. Formation of Poly(lactide) with Controlled Molecular Weight. Polymerization of Lactide by Aluminum Porphyrin. *Chem. Lett.* **1987**, *16*, 991–994.
- (14) Chamberlain, B. M.; Cheng, M.; Moore, D. R.; Ovitt, T. M.; Lobkovsky, E. B.; Coates, G. W. Polymerization of Lactide with Zinc and Magnesium b-Diiminate Complexes: Stereocontrol and Mechanism. *J. Am. Chem. Soc.* **2001**, *123*, 3229–3238.
- (15) Jones, G. O. Contributions of quantum chemistry to the development of ring opening polymerizations and chemical recycling. *Tetrahedron* **2019**, *75*, 2047–2055.
- (16) Bertini, I.; Luchinat, C.; Parigi, G. Chapter 8 Two-Dimensional Spectra and Beyond. *Current Methods in Inorganic Chemistry* **2001**, *2*, 263–302.
- (17) Lu, J.; Ma, D.; Hu, J.; Tang, W.; Zhu, D. Nuclear Magnetic Resonance Spectroscopic Studies of Pyridine Methyl Derivatives Binding to Cytochrome C. J. Chem. Soc., Dalton Trans. 1998, 2267–2273.
- (18) Marshall, E. L.; Gibson, V. C.; Rzepa, H. S. A Computational Analysis of the Ring-Opening Polymerization of rac-Lactide Initiated by Single-Site Diketiminate Metal Complexes: Defining the Mechanistic Pathway and the Origin of Stereocontrol. *J. Am. Chem. Soc.* 2005, 127, 6048–6051.
- (19) Fang, J.; Yu, I.; Mehrkhodavandi, P.; Maron, L. Theoretical Investigation of Lactide Ring-Opening Polymerization Induced by a Dinuclear Indium Catalyst. *Organometallics* **2013**, *32*, 6950–6956.
- (20) Xu, T.-Q.; Yang, G.-W.; Liu, C.; Lu, X.-B. Highly Robust Yttrium Bis(phenolate) Ether Catalysts for Excellent Isoselective Ring-Opening Polymerization of Racemic Lactide. *Macromolecules* **2017**, *50*, 515–522.
- (21) Stasiw, D. E.; Luke, A. M.; Rosen, T.; League, A. B.; Mandal, M.; Neisen, B. D.; Cramer, C. J.; Kol, M.; Tolman, W. B. Mechanism of the Polymerization of rac-Lactide by Fast Zinc Alkoxide Catalysts. *Inorg. Chem.* **2017**, *56*, 14366–14372.
- (22) Fang, J.; Tschan, M. J.-L.; Roisnel, T.; Trivelli, X.; Gauvin, R. M.; Thomas, C. M.; Maron, L. Yttrium catalysts for syndioselective b-butyrolactone polymerization: on the origin of ligand-induced stereoselectivity. *Polym. Chem.* **2013**, *4*, 360–367.
- (23) Ligny, R.; Hanninen, M. M.; Guillaume, S. M.; Carpentier, J. F. Steric vs. electronic stereocontrol in syndio- or iso-selective ROP of functional chiral beta-lactones mediated by achiral yttrium-bi-sphenolate complexes. *Chem. Commun.* **2018**, *54*, 8024–8031.